Energy efficient conversion system of a distributed solar photovoltaic station with power filtration function

Nerubatskyi Volodymyr[1], Plakhtii Oleksandr[1], Tsybulnyk Vladyslav[1], Philipjeva Maryna[1], Korneliuk Serhii[2]
Faculty of Mechanics and Energy [1] – Ukrainian State University of Railway Transport, Ukraine
Faculty of Power Supply and City Lighting [2] – O. M. Beketov National University of Urban Economy in Kharkiv, Ukraine
NVP9@i.ua, a.plakhtiy1989@gmail.com

Abstract: *The structural scheme of the distributed power supply system with the use of solar photovoltaic stations is presented. An algorithm for the conversion of a solar photovoltaic power plant conversion system in the Matlab software environment has been developed and implemented, which allows using a standard power topology to simultaneously implement two operating modes – renewable energy generation to the mains and mains current shape correction.*
***KEYWORDS**: PHOTOELECTRIC STATION, POWER SUPPLY SYSTEM, POWER FILTRATION, POWER THEORY, POWER FACTOR.*

1. Introduction

Significant interest in local power supply systems, whose consumers use renewable energy in parallel with the power grid, determines the list of issues related to the creation of electromagnetically compatible converter systems adapted to changes in operating modes and load parameters [1, 2]. Simultaneous use of several converters to implement these functionalities, such as an inverter and a power active filter, is not always economically justified. Therefore, the solution of such complex problems should be considered through the creation of new energy-efficient control algorithms for semiconductor converters with standard topological structures [3, 4].

The operation of photovoltaic solar stations in parallel with the mains is regulated by standards for the quality of electricity at the point of connection. In local power supply facilities, this problem is most acute due to the impact not only of the solar power plant, but also the modes of operation of the consumer on the quality of electricity [5, 6]. Most mains power inverters on the market of converter equipment for photovoltaic plants are not designed to solve this complex problem [7, 8]. This is a significant disadvantage of underutilization of the converter equipment, because the topologies of the power part of the transistor voltage inverter and the power active filter coincide.

Solar photovoltaic plants are becoming widespread in both the industrial and domestic sectors. Increasingly, photovoltaic stations with a nominal capacity of tens or hundreds of kilowatts appear nearby or on the territory of industrial enterprises [9, 10]. Among the objects of power supply can be distinguished a group of industrial power consumers of significant capacity, characterized by stationary modes of operation. The load schedule of such consumers changes slowly over time. These power supplies usually cause distortion of the power supply settings. To eliminate their impact on the network and the work of other consumers use passive and active filter-compensating devices. On the other hand, the converter equipment of photovoltaic solar power plants is usually selected with a certain margin for current and voltage and is designed to operate in maximum generation mode, which corresponds to the maximum solar insolation for the climate zone where the power plant will operate. For a temperate climate zone during the year, the maximum solar insolation is achieved in isolated cases, which indicates the potential for additional use of conversion equipment as a filter-compensating device [11, 12].

2. Block diagram of the power supply system

The block diagram of the distributed power supply system using solar photovoltaic stations is shown in Fig. 1.

The circuit is composed on a modular principle, consisting of a certain number of cells (*Module 1 – Module N*). Each module is formed by connecting a power load, such as a technological industrial installation with a frequency-controlled electric drive and a solar photovoltaic station. The rated load capacity of each unit is greater than the rated capacity of the power plant (*PLn* > *Psbn*). Consider the structure of the first module. The converter of the frequency-regulated electric drive is connected to the busbars of the secondary winding of the mains transformer *T* (10 / 0.4 kV) through the inductive choke *Ls1* and the uncontrolled rectifier *DR1*. The first harmonic of the mains load current of each phase is shifted relative to the corresponding phase voltage by an angle φ. In the spectrum of the mains current there are higher harmonics, multiple pulses of the rectifier $n = 6k \pm 1$, where $k = 1, 2, 3\ldots$ is the number of the harmonic current. The combined electromagnetic effect of the load units of all modules distorts the sinusoidal shape of the voltage at the input of the transformer *T*.

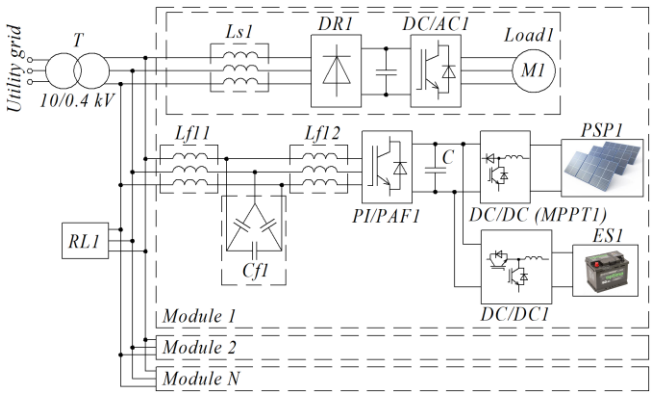

***Fig. 1.** Block diagram of the power supply system*

The solar photovoltaic station is based on an array of photovoltaic modules *PSP1*, energy-intensive storage *ES1*, capacitor *C1*, hybrid inverter *VI1* and *L-C-L* output filter, which is formed by connecting capacitor batteries *Cf1* in the gap inductive chokes *Lf1-L*. A responsible load (*RL*) is additionally connected to the common power bus. The converter system of the power plant consists of a step-up pulse converter, which performs the function of tracking the maximum power point (*MPPT1*), battery charge converter (*DC / DC1*) and voltage inverter (*PI / PAF1*). Part of the power circuit of the converter system from the capacitor bank in the DC circuit to the power supply network structurally corresponds to the parallel circuit automatic control system (ACS).

Distributed power supply system with a solar photovoltaic plant according to the structural scheme under consideration, is able to implement the following modes of operation:

– energy generation by the photovoltaic station to the power supply network under stable operation of power and responsible load;

– power filtration of mains current with stable operation of power and responsible load;

– energy generation by the photovoltaic station to the power supply network with simultaneous filtration of the mains current with stable operation of the power and responsible load;

– autonomous power supply of the responsible load from the photovoltaic station;

– autonomous power supply of the responsible load with partial power supply of the power load from the photovoltaic station.

Additional modes of operation of the distributed power supply system under consideration are the modes associated with the use of energy-intensive storage of photovoltaic power plants to equalize the daily load schedule of the transformer station with stable operation of power and responsible load.

The multifunctionality of the transformer system of a distributed solar power plant is realized on the basis of an algorithm based on the transformations of the modified *p-q-r* power theory [13, 14]. The block diagram of the control system, which explains the operation of the algorithm, is shown in Fig. 2.

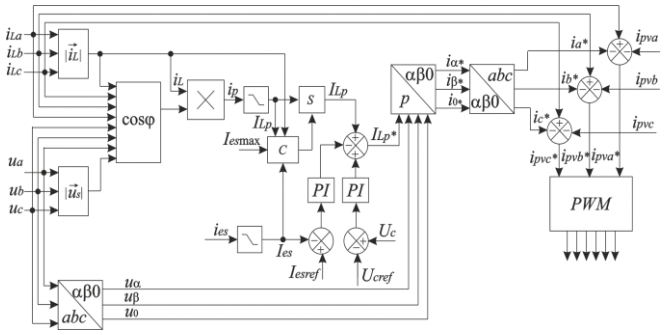

Fig. 2. *Block diagram of the control system of the conversion system*

The block diagram follows the principle of forming problems by phase currents after standard transformations of *p-q-r* theory coordinate systems and provisions of cross-vector theory, except for adding a separate node with feedback on the constant component of the discharge current of the drive I_{es}. The input of the control system receives signals from the voltage sensors installed on the low voltage buses of the transformer u_a, u_b, u_c, and load current sensors i_{La}, i_{Lb}, i_{Lc}. Above the signals received from the voltage sensors, standard Clarke transformations from Cartesian *abc* to *αβ0* coordinates are performed.

Using the provisions of cross-vector power theory, the modules of the spatial vectors of the mains voltage and load current, as well as the cosine of the shear angle between these vectors by ratios are calculated.

Multiplying the modulus of the load current vector by the value of the cosine of the shear angle allows to calculate the value of the modulus of the load current vector along the axis *p* of the spatial rotating Cartesian system *p-q-r* [15]:

$$i_{Lp} = i_L \cdot \cos\varphi. \tag{1}$$

At sinusoidal symmetrical voltages of the power supply network, the direction of the vector i_{Lp} coincides with the direction of the vector u_s.

After averaging the current trajectory i_{Lp} on the period of recurrence *T* we obtain the average value of the load current along the axis *p*:

$$I_{Lp} = \frac{1}{T}\int_{t}^{t+T} i_{Lp}dt \tag{2}$$

which corresponds to a constant flow of energy from the power supply to the load.

The input of the switch *S*, which is switched by the comparator *C*, receives an average signal of the load stump along the axis *p*.

In the combined mode of operation of the photovoltaic plant and ACS, the reference signal on the current vector along the axis *p* is formed by three virtually independent components: the DC current component I_{Lp} along the axis *p*, the mismatch of the voltage signal on the capacitor in the DC circuit relative to the task (U_c*) and signal mismatch drive relative to the task current (I_{es}*). The first two signals are typical for the operation of the ACS, and the third signal – for the operation of the inverter.

If the power plant operates in the mode close to the maximum generation, the input of the task unit receives a signal on the generation current only from the last controller, ie the converter works as a standard mains inverter, giving energy to the industrial network [16, 17].

$$\sqrt{I_{es}^2 + I_c^2} \le I_{es\max}, \tag{3}$$

where I_{es} – the current generation current corresponding to the discharge current of the drive; I_{sbmax} – maximum generation current.

As soon as inequality (3) is executed, the compensator current, the comparator *C* is switched and the task signal for the compensator currents is added to the task signal by the generation current:

$$I_c = \sqrt{\frac{1}{T}\int_{t}^{t+T}\left(i_L^2 - I_{Lp}^2\right)dt}, \tag{4}$$

The value of the maximum generation current is limited by the characteristics of the transistor modules of the output inverter [18, 19].

The calculated components are current problems along the axis *p* in the spatial coordinate system *p-q-r*. To receive them at the input of the PWM-generator, need to perform two inverse coordinate transformations: $p \rightarrow \alpha\beta 0$:

$$\begin{bmatrix} i_\alpha^* \\ i_\beta^* \\ i_0^* \end{bmatrix} = \frac{I_{Lp}^*}{u_{\alpha\beta 0}} \begin{bmatrix} u_\alpha \\ u_\beta \\ u_0 \end{bmatrix}, \tag{5}$$

and inverse transformation Clarke $\alpha\beta 0 \rightarrow abc$:

$$\begin{bmatrix} i_a^* \\ i_b^* \\ i_c^* \end{bmatrix} = \sqrt{\frac{2}{3}} \cdot \begin{bmatrix} 1 & 0 & -\frac{1}{\sqrt{3}} \\ -\frac{1}{2} & \frac{\sqrt{3}}{2} & \frac{1}{\sqrt{2}} \\ -\frac{1}{2} & -\frac{\sqrt{3}}{2} & \frac{1}{\sqrt{2}} \end{bmatrix} \cdot \begin{bmatrix} i_\alpha^* \\ i_\beta^* \\ i_0^* \end{bmatrix}. \tag{6}$$

After phase-by-phase subtraction of the task currents from the load currents, taking into account the feedback on the power plant currents, we obtain the task signals on the power plant currents:

$$\begin{bmatrix} i_{pva}^* \\ i_{pvb}^* \\ i_{pvc}^* \end{bmatrix} = \begin{bmatrix} i_{La} - i_a^* - i_{pva} \\ i_{Lb} - i_b^* - i_{pvb} \\ i_{Lc} - i_c^* - i_{pvc} \end{bmatrix}. \tag{7}$$

3. Simulation of the Microgrid system in the Matlab software environment

To test the control algorithm of the converter system of a solar photovoltaic station, which is able to implement multifunctional modes of operation of the power supply system, a Matlab model of a distributed power supply system was synthesized (Fig. 3).

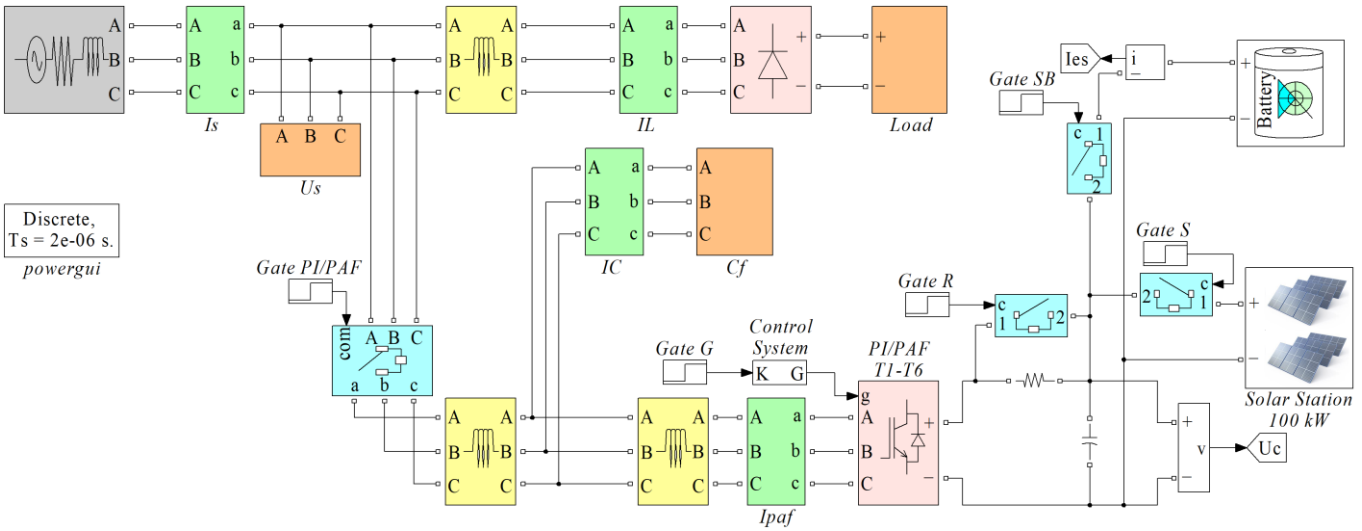

Fig. 3. *Matlab-model of a distributed power supply system with a solar power plant*

The scheme of the power supply system corresponds to the block diagram in Fig. 1 and is a three-phase three-wire network of sinusoidal voltages (effective value of linear voltage – U_l = 380 V, frequency – f = 50 Hz, inductance – L_s = 28 μH, active resistance – R_s = 0.36 Ω), from which through a constant circuit the current generated by the three-phase uncontrolled rectifier is fed by a frequency-regulated drive with a nominal power of P_{LH} = 300 kW with the inductance of the inlet reactor L_d = 75 μH. At the points of joint connection of loads through the power three-phase voltage inverter, the solar photovoltaic station Solar Station is connected to the network with nominal power P_{sbH} = 100 kW (voltage in the DC circuit – U_c = 770 V; input capacitor capacity – C = 0.594 mF; output filter inductance – L_{f1} = 21 μH, L_{f2} = 21 μH, the capacity of the output filter – C_f = 36,8 μF).

The structure of a solar power plant is based on a detailed mathematical model of a photocell, the set of which forms a solar photomodule with real technical characteristics. The connection of the same type of photomodules forms a photoelectric array.

The voltage inverter is made according to the bridge circuit on IGBT modules with reverse diodes [20]. Battery and input filter capacitor are connected to the converter circuit (rated voltage – U_{esH} = 670 V; rated capacity – C_H = 300 Ah; maximum capacity – $C_{\max}$ = 300 Ah; full charge voltage – U_{fc} = 779 V; rated discharge current – I_{ds} = 130 A, internal resistance – R_{es} = 0.0223 Ω). On the side of the three-phase power supply, an output filter is connected, which is formed by two sections of inductive reactor batteries, in the gap of which a capacitor battery C_f is connected, the phases of which are united in a "triangle".

The performance of the proposed algorithm can be verified by performing a sequential transition from the uncompensated mode of operation of the consumer to the compensated, and then to the integrated mode, which combines the operation of the ACS and the energy generation of the renewable source.

Operating oscillograms obtained in steady state for each of the three options for the operation of a distributed power supply system are shown in Fig. 4.

In Fig. 4, a and it is seen that the uncompensated load current has a non-sinusoidal shape characteristic of the operation of an uncontrolled three-phase rectifier.

After the ACS connection, the shape of the phase current is almost sinusoidal and coincides in phase with the corresponding voltage (Fig. 4, b).

After connecting a solar photovoltaic station, the amplitude of the first harmonic of the mains phase current decreases in proportion to the discharge current of the storage I_{es} (Fig. 4, c), which indicates the combined power supply load from the network and the solar power plant.

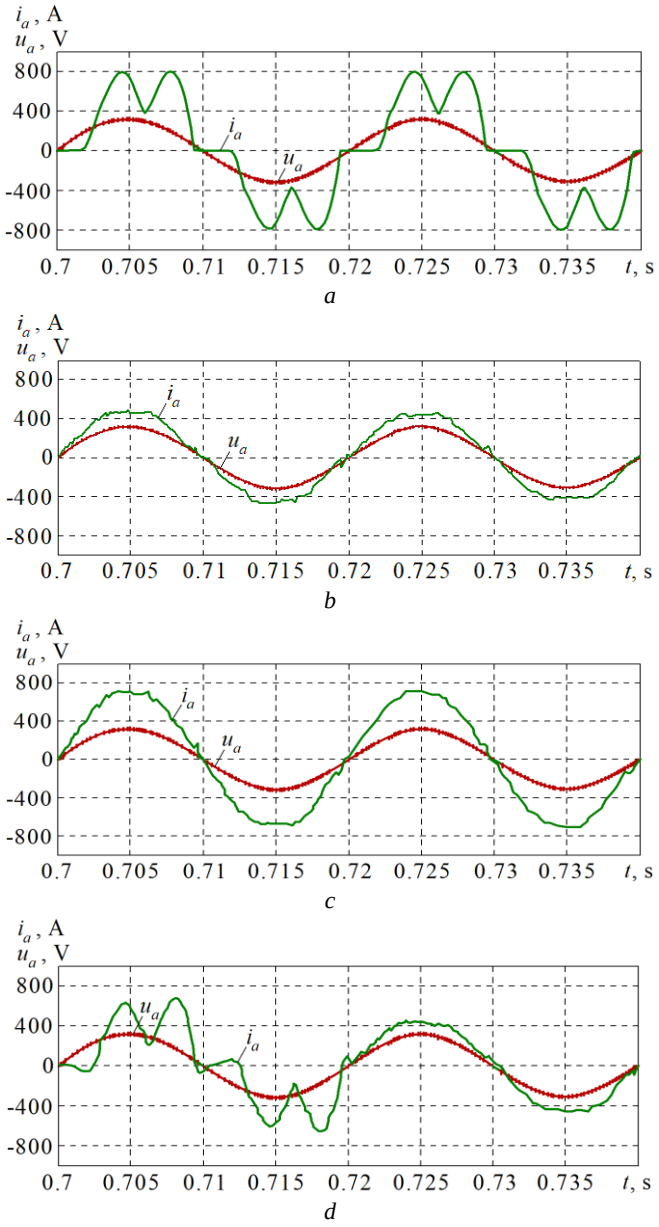

Fig. 4. *Oscillograms of mains voltage and current phase A:*
a – uncompensated load current; b – ACS connection;
c – connection of a solar photovoltaic station;
d – load current compensation mode

The THD of the rectifier without the correction mode and with the power factor correction mode is shown in Fig. 5.

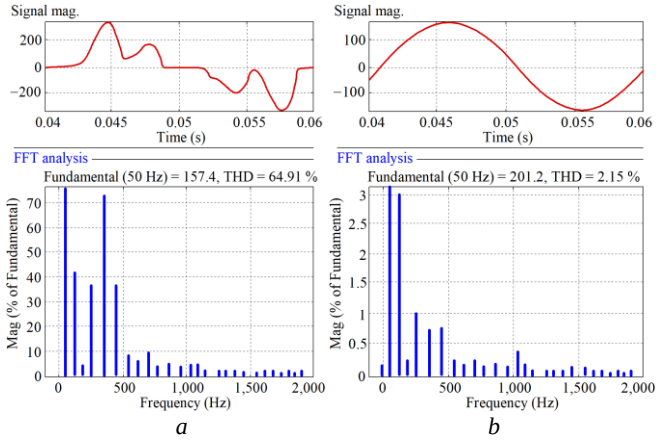

a *b*

Fig. 5. *THD rectifier:*
a – without power factor correction mode;
b – with power factor correction mode

According to the simulation results, the combined operation of two regulators – the voltage regulator on the capacitor and the current regulator of the storage discharge has little effect on their stability due to the fact that the voltage on the capacitor is maintained by a constant additional charge controller. If equation (1) is executed in the generation mode, then the comparator is switched and the load current compensation mode is added to the generation mode (Fig. 4, d).

4. Results and discussion

An algorithm for the conversion of a solar photovoltaic power plant conversion system has been developed and implemented in the Matlab / Simulink software environment. When implementing the algorithm, the use of a modified *p-q-r* theory of power is proposed, which allowed to significantly reduce the number of calculations of the microcontroller system of autoregulation.

5. Conclusion

Verification of the algorithm on the synthesized simulation model of the cell of the distributed power supply system confirms the correctness in a wide range of changes in the parameters of the load and the generation current of the renewable source.

6. References

1. Klug R. D., Klaassen N. Highpower medium voltage drives – innovation, portfolio, trends. *Power Electronics and Applications. 2005 IEEE European Conference*. 2005. P. 1–10.

2. Ortjohann E., Mohd A., Hamsic N., Morton D., Omari O. Advanced control strategies for three-phase grid inverters with unbalanced loads for pv/hybrid power systems. *21st European Photovoltaic Solar Energy Conference*. 2006. P. 1–7.

3. Nerubatskyi V., Plakhtii O., Hordiienko D., Khoruzhevskyi H. Study of energy parameters in alternative power source microgrid systems with multi-level inverters. *International scientific journal «Industry 4.0»*. 2020. Vol. 5, Issue 3. P. 118–121.

4. Nerubatskyi V. P., Plakhtii O. A., Karpenko N. P., Hordiienko D. A., Tsybulnyk V. R. Analysis of energy processes in a seven-level autonomous voltage inverter at various modulation algorithms. *Information and Control Systems at Railway Transport*. 2019. No. 5. P. 8–18. DOI: 10.18664/ikszt.v24i5.181286.

5. Tsao-Tsung M. Power Quality Enhancement in Micro-grids Using Multifunctional DG Inverters. *Proceedings of the International MultiConference of Engineers and Computer Scientists*. 2012. Vol. II. P. 996–1001.

6. Nerubatskyi V. P., Plakhtii O. A., Tsybulnyk V. R., Hordiienko D. A., Khoruzhevskyi H. A. Analysis of energy efficiency indicators of autonomous voltage inverters with impedance and quasi-impedance links in the input circuit using different modulation algorithms. *Information and Control Systems at Railway Transport*. 2020. No. 3. P. 19–31. DOI: 10.18664/ikszt.v25i3.214089.

7. Inverter for a three-phase AC photovoltaic system. Hinman B., Kazemi H., Miller W. U. S. Patent 8,618,456. Issued December 31, 2013.

8. Akagi H., Vatanabe E. H., Aredes M. Instantaneous power theory and applications to power conditioning. *IEEE Press Willy-Interscience*. 2007. P. 379.

9. Zhemerov G. G., Krylov D. S., Tugay D. V. Verification of the calculation of elements and quality indicators of the power supply system with a parallel active power filter. *Bulletin of the National Technical University "Kharkiv Polytechnic Institute"*. 2015. Vol. 12. P. 394-397.

10. Depenbrock M., Staudt V., Wrede H. Concerning instantaneous power compensation in three-phase systems by using p-q-r theory. *IEEE Trans. Power. Electron*. 2004. Vol. 19. No. 4. P. 1151–1152.

11. Nerubatskyi V., Plakhtii O., Ananieva O., Zinchenko O. Analysis of the Smart Grid concept for DC power supply systems. *International scientific journal «Industry 4.0»*. 2019. Vol. 4, Issue 4. P. 179–182.

12. Lee S., Kim H., Sul S., Blaabjerg F. A novel control algorithm for static series compensators by use of PQR instantaneous power theory. *IEEE Trans. Power Electron*. 2004. Vol. 19. No. 3. P. 814–827.

13. Kim H., Blaabjerg F., Bak-Jensen B., Choi I. Instantaneous power compensation in three-phase systems using p-q-r theory. *IEEE Trans. Power Electronics*. 2002. Vol. 17. No. 5. P. 701–710.

14. Ng F., Vong M., Han Y. Analysis and control of UPQS and its DC-link power by use of p-q-r instantaneous power theory. *1st Int. Conf. Power Electron. Syst. Appl*. 2004. P. 43–53.

15. Kim H., Blaabjerg F., Bak-Jensen B., Choi I. Instantaneous power compensation in three-phase systems using p-q-r theory. *IEEE Trans. Power Electronics*. 2002. Vol. 17. No. 5. P. 701–710.

16. Peng F., Ott G., Adams D. Harmonic and reactive power compensation based on the generalized instantaneous reactive power theory for three-phase four-wire systems. *IEEE Trans. Power Electronics*. 1998. Vol. 13. No. 6. P. 1174–1181.

17. Polishchuk S. Y., Artemenko M. Yu., Mikhalsky V. M. Analysis of construction of coordinate systems in the theory of instantaneous power of three-phase circuits for control of active filtration devices. *Technical electrodynamics*. 2013. No. 2. P. 25–35.

18. Plakhtii O. A., Nerubatskyi V. P., Hordiienko D. A., Khoruzhevskyi H. A. Calculation of static and dynamic losses in power IGBT-transistors by polynomial approximation of basic energy characteristics. *Scientific bulletin of National mining university*. 2020. No. 2 (176). P. 82–88. DOI: 10.33271/nvngu/2020-82.

19. Polishchuk S. Y. Increase of electromagnetic compatibility of semiconductor energy converters with a power supply network by means of management and active filtration: Dis. for the degree of Cand. those. science: 05.09.12. 2013. 250 c.

20. Plakhtiy A., Nerubatskyi V., Tsybulnyk V. Stabilization of voltages on capacitors of cells in modular multilevel inverters with space-vector PWM. *Bulletin of NTU «KhPI». Series: Electrical Machines and Electromechanical Energy Conversion*. 2019. No. 20 (1345). P. 42–52. DOI: 10.20998/2409-9295.2019.20.06.